Published in final edited form as:
Circulation. 2010 April 13; 121(14): 1606–1613. doi:10.1161/CIRCULATIONAHA.109.914911.

Elevated Cytosolic Na^+ Increases Mitochondrial Formation of Reactive Oxygen Species in Failing Cardiac Myocytes

Michael Kohlhaas, PhD, **Ting Liu, PhD**, **Andreas Knopp, PhD**, **Tanja Zeller, PhD**, **Mei Fang Ong, PhD**, **Michael Böhm, MD**, **Brian O'Rourke, PhD**, and **Christoph Maack, MD**
the Klinik für Innere Medizin III (M.K., A.K., T.Z., M.B., C.M.) and Institut für Medizinische Biometrie (M.F.O.), Epidemiologie und Medizinische Informatik, Universitätsklinikum des Saarlandes, Homburg, Germany; and The Johns Hopkins University (T.L., B.O.), Institute of Molecular Cardiobiology, Baltimore, Md.

Abstract

Background——Oxidative stress is causally linked to the progression of heart failure, and mitochondria are critical sources of reactive oxygen species in failing myocardium. We previously observed that in heart failure, elevated cytosolic Na^+ ($[Na^+]_i$) reduces mitochondrial Ca^{2+} ($[Ca^{2+}]_m$) by accelerating Ca^{2+} efflux via the mitochondrial Na^+/Ca^{2+} exchanger. Because the regeneration of antioxidative enzymes requires NADPH, which is indirectly regenerated by the Krebs cycle, and Krebs cycle dehydrogenases are activated by $[Ca^{2+}]_m$, we speculated that in failing myocytes, elevated $[Na^+]_i$ promotes oxidative stress.

Methods and Results——We used a patch-clamp–based approach to simultaneously monitor cytosolic and mitochondrial Ca^{2+} and, alternatively, mitochondrial H_2O_2 together with NAD(P)H in guinea pig cardiac myocytes. Cells were depolarized in a voltage-clamp mode (3 Hz), and a transition of workload was induced by β-adrenergic stimulation. During this transition, NAD(P)H initially oxidized but recovered when $[Ca^{2+}]_m$ increased. The transient oxidation of NAD(P)H was closely associated with an increase in mitochondrial H_2O_2 formation. This reactive oxygen species formation was potentiated when mitochondrial Ca^{2+} uptake was blocked (by Ru360) or Ca^{2+} efflux was accelerated (by elevation of $[Na^+]_i$). In failing myocytes, H_2O_2 formation was increased, which was prevented by reducing mitochondrial Ca^{2+} efflux via the mitochondrial Na^+/Ca^{2+} exchanger.

Conclusions——Besides matching energy supply and demand, mitochondrial Ca^{2+} uptake critically regulates mitochondrial reactive oxygen species production. In heart failure, elevated $[Na^+]_i$ promotes reactive oxygen species formation by reducing mitochondrial Ca^{2+} uptake. This novel mechanism, by which defects in ion homeostasis induce oxidative stress, represents a potential drug target to reduce reactive oxygen species production in the failing heart.

Keywords

heart failure; sodium; calcium; free radicals; ion channels

Correspondence to Christoph Maack, MD, Universitätsklinikum des Saarlandes, Klinik für Innere Medizin III, 66421 Homburg, Germany. maack@gmx.org.

The online-only Data Supplement is available with this article at http://circ.ahajournals.org/cgi/content/full/CIRCULATIONAHA.109.914911/DC1.

Disclosures
None.

Oxidative stress plays a fundamental role in many cardiovascular diseases and aging.[1,2] In chronic heart failure, oxidative stress is causally linked to the progression of the disease,[1,3,4] and mitochondria were identified as critical sources of reactive oxygen species (ROS) in the heart.[5] ROS impair excitation-contraction (EC) coupling,[6–8] cause arrhythmias,[9] and contribute to cardiac remodeling by activating signaling pathways that induce hypertrophy, apoptosis, and necrosis.[10–13] The precise mechanisms that regulate mitochondrial ROS formation, however, are incompletely understood.

In cardiac myocytes, the processes of EC coupling consume large amounts of ATP, which is replenished by oxidative phosphorylation in mitochondria. Because the heart undergoes frequent changes in workload, precise matching of ATP supply and demand is essential to maintain cardiac function.[14] Two key regulators of oxidative phosphorylation are ADP and Ca^{2+}. When energy consumption increases (eg, during β-adrenergic stimulation), elevated ADP stimulates ATP production at the F_1/F_0-ATPase (Figure 1). This accelerates electron flux along the electron transport chain (ETC) and oxidizes the primary electron donor, NADH. To maintain the higher electron fluxes, a concomitant increase in NADH production must occur. This is accomplished by Ca^{2+}-induced stimulation of rate-controlling dehydrogenases of the Krebs cycle.[15–17] Ca^{2+} enters mitochondria via a Ca^{2+} uniporter (MCU) and is exported by a Na^+/Ca^{2+} exchanger (mNCE). Although the kinetics of mitochondrial Ca^{2+} uptake are still debated (ie, slow uptake versus beat-to-beat oscillations), most studies agree that in response to an elevation of the frequency or amplitude of cytosolic Ca^{2+} transients (as occurs during β-adrenergic stimulation), steady state mitochondrial $[Ca^{2+}]$ ($[Ca^{2+}]_m$) increases.[16] Thus, energy supply and demand matching is closely linked to the processes of EC coupling.

In chronic heart failure, perturbations of EC coupling cause contractile dysfunction.[18,19] One major deficit is a decreased Ca^{2+} load of the sarcoplasmic reticulum, which reduces cytosolic Ca^{2+} transients.[18,19] On the other hand, the cytosolic Na^+ concentration ($[Na^+]_i$) is elevated, which facilitates cytosolic Ca^{2+} influx via the sarcolemmal Na^+/Ca^{2+} exchanger during the action potential.[20–23] Although this compensates in part for the decreased sarcoplasmic reticulum Ca^{2+} load, we previously reported that an elevation of $[Na^+]_i$ negatively affects energy supply and demand matching.[17,24] Because mitochondrial Ca^{2+} efflux is governed by a Na^+/Ca^{2+} exchanger (mNCE), elevation of $[Na^+]_i$ accelerates mitochondrial Ca^{2+} efflux, and reduced $[Ca^{2+}]_m$ hampers the activation of Krebs cycle dehydrogenases. This results in pronounced oxidation of NADH to NAD^+ during transitions of workload.[17,24]

Besides its elemental role in the regulation of oxidative phosphorylation via NADH, the Krebs cycle may also play a key role in recovery of the antioxidative capacity of the mitochondrial matrix. Under physiological conditions, 0.2% to 2% of oxygen is incompletely reduced to superoxide ($^{\bullet}O_2^-$) at the ETC, which is then dismutated to H_2O_2 by the matrix-located superoxide dismutase.[2] H_2O_2, in turn, is eliminated by peroxiredoxin and glutathione peroxidase,[2] and the regeneration of these enzymes requires reduced NADPH (Figure 1).[25,26] Oxidized $NADP^+$ is recovered to NADPH by $NADP^+$-dependent isocitrate dehydrogenase, $NADP^+$-dependent malic enzyme, and nicotinamide nucleotide transhydrogenase.[25] Considering that all 3 NADPH-regenerating enzymes derive their substrates from the Krebs cycle (isocitrate, malate, and NADH; Figure 1), and the turnover rate of the Krebs cycle is regulated by Ca^{2+}, we hypothesized that during transitions of workload, mitochondrial Ca^{2+} uptake maintains the antioxidative capacity of the matrix in a reduced state and thus controls mitochondrial levels of H_2O_2.

Using a patch-clamp based approach, we observed that during transitions of workload, transient oxidations of NAD(P)H were associated with increased formation of mitochondrial H_2O_2, whereas mitochondrial Ca^{2+} uptake recovered NAD(P)H and decreased H_2O_2 formation. In failing myocytes, elevated $[Na^+]_i$ reduced mitochondrial Ca^{2+} uptake and potentiated

mitochondrial H_2O_2 formation. The results reveal a novel mechanism by which defects in cellular Na^+ homeostasis induce mitochondrial oxidative stress in the failing heart.

Methods

A detailed Methods section can be found in the online-only Data Supplement.

Heart Failure Model and Functional Evaluation

Aortic banding was performed in guinea pigs as described previously.[24] Animals underwent echocardiography every 2 weeks after surgery. Left ventricular ejection fraction was calculated with VisualSonics V1.3.8 software from 2-dimensional long-axis views. When a decrease in ejection fraction was observed, animals were euthanized, heart weight/body weight was measured, and cardiomyocytes were isolated.

Cell Isolation

Cardiac myocytes were isolated from normal and failing guinea pig hearts by enzymatic digestion and stored in supplemented Dulbecco's modified Eagle's medium (Invitrogen, Karlsruhe, Germany) as described previously.[17,24]

Patch-Clamp Experiments

Myocytes were voltage clamped in the whole-cell configuration (37°C, pipette resistance 2 to 4 MΩ) and equilibrated with a physiological K^+-glutamate–based pipette solution as described previously.[17,24] For the experiments in Figures 2 through 5, myocytes were depolarized from −80 to 10 mV at 3 Hz for 80 ms, and isoproterenol (10 and 100 nmol/L) was used to increase workload via β-adrenergic stimulation. To inhibit the MCU, Ru360 (1 μmol/L) was added to the pipette solution. Alternatively, $[Na^+]$in the pipette solution was raised from 5 to 15 mmol/L to accelerate mitochondrial Ca^{2+} efflux via the mNCE.[17] For the protocol in Figure 6D, myocytes were depolarized at 4 Hz for 3 minutes in the presence of isoproterenol (100 nmol/L) as described previously.[24]

Fluorescence Recordings to Determine $[Ca^{2+}]_c$, $[Ca^{2+}]_m$, NAD(P)H, and H_2O_2

To monitor $[Ca^{2+}]_c$ together with $[Ca^{2+}]_m$, myocytes were loaded with the cell-permeable Ca^{2+} indicator rhod-2 acetoxymethyl esther (rhod-2 AM, 3 μmol/L; Invitrogen), which locates primarily to mitochondria, and then dialyzed with a pipette solution that contained indo-1 salt to monitor $[Ca^{2+}]_c$, as described previously.[17] Alternatively, myocytes were loaded with the H_2O_2-sensitive 5-(-6)-chloromethyl-2′,7′-dichlorohydrofluorescein diacetate (CM-H_2DCFDA; Invitrogen), which locates primarily to mitochondria,[27] and dialyzed with dye-free pipette solution. The fluorescent product CM-DCF was monitored together with the autofluorescence of NAD(P)H (online-only Data Supplement Figures I through III).

Field Stimulation in Failing and Nonfailing Myocytes

For the experiments in Figure 6C, myocytes were field stimulated in a heated chamber (37°C) at 4 Hz in the presence of isoproterenol as described previously,[24] and H_2O_2 formation was recorded by CM-DCF fluorescence in the absence and presence of CGP-37157 (1 μmol/L), respectively.

Statistical Analysis

Values are given as mean±SEM. Statistical analysis was performed with 2-way ANOVA (Figures 2F and 2G) and 1-way (Figures 4B through 4D, 5C, 6C, and 6D) or 2-way (Figure 2C) ANOVA for repeated measures, respectively. An unpaired or paired *t* test was applied for Figures 6A and 6B, respectively, and linear regression analysis was applied in Figures 3F and

4E. Analysis was performed with SPSS (ANOVA) and GraphPad Prism (*t* tests, regression analysis; version 3.00 for Windows, GraphPad Software; San Diego, Calif).

Results

Beat-to-Beat Oscillation of $[Ca^{2+}]_m$ During Cytosolic Ca^{2+} Transients

Guinea pig myocytes were voltage clamped and depolarized at 3 Hz. Isoproterenol increased the L-type Ca^{2+} current ($I_{Ca,L}$) and the amplitude of cytosolic Ca^{2+} transients ($\Delta[Ca^{2+}]_c$; Figures 2A and 2B). During cytosolic Ca^{2+} transients, rapid mitochondrial Ca^{2+} transients were recorded (Figure 2C), with a linear relationship between $\Delta[Ca^{2+}]_m$ and $\Delta[Ca^{2+}]_c$ (Figure 2D). The time to peak of $[Ca^{2+}]_m$ was shorter than that of $[Ca^{2+}]_c$, whereas the decay of $[Ca^{2+}]_m$ was slower than that of $[Ca^{2+}]_c$ (Figures 2E through 2G). When $\Delta[Ca^{2+}]_c$ increased, diastolic $[Ca^{2+}]_m$ accumulated, whereas diastolic $[Ca^{2+}]_c$ was maintained (Figures 2B and 2C). The addition of Ru360, a selective inhibitor of the MCU,[28] to the pipette solution reduced $\Delta[Ca^{2+}]_m$ by approximately two thirds and prevented diastolic accumulation of $[Ca^{2+}]_m$ (Figures 2C through 2E). Conversely, $[Ca^{2+}]_c$ was slightly (although insignificantly) increased by Ru360. Time to peak of $[Ca^{2+}]_m$, but not of $[Ca^{2+}]_c$, was prolonged by Ru360, whereas the decays of $[Ca^{2+}]_m$ and $[Ca^{2+}]_c$ were unchanged.

Dynamic Regulation of Mitochondrial H_2O_2 by $[Ca^{2+}]_m$ and NAD(P)H

To relate the changes in $[Ca^{2+}]_c$ and $[Ca^{2+}]_m$ to the mitochondrial redox state of NAD(P)H/$NAD(P)^+$ and ROS production, we determined the autofluorescence of NAD(P)H while monitoring the mitochondrial oxidation rate of an H_2O_2-sensitive probe (CM-DCF; Figures 3D and 3E; online-only Data Supplement Figures I through III). This probe will sense the balance between H_2O_2 production and scavenging, and thus, it reports the biologically relevant amount of H_2O_2 that actually exerts its effects within or outside mitochondria. Because the experimental protocol and conditions were identical to the protocol that determined $[Ca^{2+}]_m$ and $[Ca^{2+}]_c$ (Figure 2), the amplitudes of $[Ca^{2+}]_c$ transients (Figure 3B) and changes of diastolic $[Ca^{2+}]_m$ (Figure 3C) were included in this Figure, which facilitates cross comparisons with the analysis of NAD(P)H and H_2O_2. CM-DCF oxidation increased immediately on electrical stimulation of myocytes (Figure 3E), whereas the redox state of NAD(P)H/$NAD(P)^+$ was maintained during the first 3 minutes of stimulation (Figure 3D). After β-adrenergic stimulation, when $I_{Ca,L}$ and $\Delta[Ca^{2+}]_c$ increased rapidly, NAD(P)H was oxidized within the first minute (Figures 3A, 3B, and 3D). At the same time, the rate of CM-DCF oxidation increased ≈6-fold (Figures 3E and 3G). The degrees of NAD(P)H and CM-DCF oxidation both correlated with the absolute increase of $I_{Ca,L}$ within the first 30 seconds after isoproterenol exposure (r=0.58 and −0.65, P<0.05, respectively; not shown). This indicates that the more abrupt the transition of workload was, the more NAD(P)H was temporarily oxidized and the more H_2O_2 increased.

The initial oxidation of NAD(P)H was followed by its continuous recovery over the next 5 minutes (Figure 3D). This recovery correlated closely with the increase in diastolic $[Ca^{2+}]_m$ (Figures 3C, 3D, and 3F), in line with the concept that $[Ca^{2+}]_m$ activates rate-controlling dehydrogenases of the Krebs cycle to accelerate the regeneration of NAD(P)H.[14–17] The rate of mitochondrial formation of H_2O_2 peaked 1 minute after application of isoproterenol (at minute 6 of the protocol), when NAD(P)H was maximally oxidized (Figure 3G). With the subsequent Ca^{2+}-induced recovery of NAD(P)H, net H_2O_2 formation decreased in parallel, reaching a new steady state at a rate comparable to the level before β-adrenergic stimulation, albeit at more reduced NAD(P)H/$NAD(P)^+$ (Figure 3G).

Blocking Mitochondrial Ca^{2+} Uptake Increases H_2O_2

To causally relate the regulation of NAD(P)H/$NAD(P)^+$ and H_2O_2 to mitochondrial Ca^{2+} uptake, the MCU was blocked by the addition of Ru360 (1 μmol/L) to the pipette solution. Despite a similar increase in $I_{Ca,L}$ and $\Delta[Ca^{2+}]_c$ after β-adrenergic stimulation (Figures 2A and 4A), the lack of mitochondrial Ca^{2+} accumulation potentiated the initial oxidation and blunted the recovery of NAD(P)H, which resulted in more oxidized NAD(P)H/$NAD(P)^+$ than in control conditions (Figures 4B and 4C). This was associated with an elevated rate of H_2O_2 formation (Figure 4D). When both groups were combined, the NAD(P)H/$NAD(P)^+$ redox state correlated positively with $[Ca^{2+}]_m$ (Figure 4E) but inversely with H_2O_2 (Figure 4F).

Elevation of $[Na^+]_i$ Increases H_2O_2

In cardiac hypertrophy and failure, $[Na^+]_i$ is elevated,[20–22] and Ca^{2+} export from mitochondria, governed by the mNCE, consequently is increased, which limits $[Ca^{2+}]_m$ accumulation and oxidizes NAD(P)H.[17,24] Thus, we speculated that elevating $[Na^+]_i$ would increase mitochondrial H_2O_2 levels. This was tested by use of a similar protocol with either 5 or 15 mmol/L $[Na^+]_i$ in the pipette solution (Figure 5). The relationship between systolic (or diastolic) $[Ca^{2+}]_m$ and the respective $[Ca^{2+}]_c$ was shifted in the direction of lower $[Ca^{2+}]_m$ per $[Ca^{2+}]_c$ at 15 versus 5 mmol/L $[Na^+]_i$ during the first 5 to 8 minutes of the protocol (Figures 5A and 5B), which indicates that elevated $[Na^+]_i$ promotes mitochondrial Ca^{2+} efflux via the mNCE.[17,24,29] At 15 mmol/L $[Na^+]_i$, H_2O_2 levels were elevated compared with 5 mmol/L $[Na^+]_i$, especially during the first 4 minutes of β-adrenergic stimulation (Figures 5C and 5D), which resembled the time frame in which the relation between $[Ca^{2+}]_m$ and $[Ca^{2+}]_c$ diverged between 5 and 15 mmol/L $[Na^+]_i$ (Figures 5A and 5B).

Deficient Mitochondrial Ca^{2+} Uptake Accounts for Increased ROS in Heart Failure

In a guinea pig model of heart failure (induced by ascending aortic banding), $[Na^+]_i$ increased from 5 to 17 mmol/L in failing versus nonfailing myocytes, and NAD(P)H oxidized in response to an abrupt increase in workload.[24] After 4 weeks, aortic banding induced left ventricular hypertrophy and contractile dysfunction in vivo (Figures 6A and 6B). Myocytes from failing hearts displayed a 20-fold increase in the rate of CM-DCF oxidation compared with control myocytes after abruptly enhancing workload in vitro (Figure 6C). This marked increase in H_2O_2 was prevented by the inhibition of the mNCE with CGP-37157 (Figure 6C), which potentiates mitochondrial Ca^{2+} accumulation in nonfailing and failing cells[17,24] and prevents NAD(P)H oxidation in failing myocytes.[24]

To corroborate the link between increased H_2O_2 formation and elevated $[Na^+]_i$, the cytosol of failing myocytes was equilibrated with pipette solutions that contained either 15 or 5 mmol/L $[Na^+]_i$ and depolarized at 4 Hz in voltage-clamp mode. Indeed, by lowering $[Na^+]_i$, H_2O_2 formation was normalized to levels that occurred in nonfailing myocytes with endogenous $[Na^+]_i$ of ≈5 mmol/L (Figure 6D).

Discussion

The main findings of the present study are that during transitions of workload, (1) transient oxidations of NAD(P)H in cardiac myocytes are associated with increased mitochondrial formation of H_2O_2, (2) mitochondrial Ca^{2+} uptake controls net H_2O_2 formation by recovering NAD(P)H through activation of Krebs cycle dehydrogenases, and (3) elevated $[Na^+]_i$ reduces mitochondrial Ca^{2+} uptake and promotes formation of H_2O_2 in failing cardiac myocytes.

Oxidative Stress in Heart Failure

Increased oxidative stress is observed in the plasma and myocardium of patients with heart failure and is related to an impairment of left ventricular function.[30–32] Indeed, animal models suggest a causal link between oxidative stress and the progression of contractile dysfunction to overt heart failure.[1,3,4] Besides NADPH oxidase, xanthine oxidase, and uncoupled nitric oxide synthases, mitochondria are important sources of ROS.[1,5,31] The relative contribution of these different sources to overall oxidative stress in the failing heart, however, is presently unknown. Owing to the short half-life and high reactivity of ROS, microdomains of ROS may exist with differential effects on cell function, depending on their subcellular localization and source. For instance, although NADPH oxidase–derived ROS are involved in the development of cardiac hypertrophy,[33,34] mitochondrial ROS induce energetic deficits,[27] apoptosis,[12] an impairment of EC coupling,[7] and arrhythmias.[9] However, the precise regulation of mitochondrial ROS production under physiological and pathological conditions, especially in intact cells, is incompletely understood.

Regulation of Mitochondrial ROS Production

In studies on isolated mitochondria, electrons leak from complexes I and III of the ETC to O_2, producing $^{\bullet}O_2^-$. A greater reduction of these complexes (for example, when NADH is highly reduced in the absence of ADP at low rates of respiration [“state 4”]) increases the probability of electron leak and ROS production.[2,35] Initiation of NADH oxidation by the addition of ADP (“state 3” respiration) or partial uncoupling of mitochondria (eg, with chemical protonophores) can decrease ROS production.[36,37] According to this model, one might expect that an increase in work (and thus, oxygen consumption) would favor a decrease of ROS levels.[2] However, this model of ROS production is largely based on the behavior of isolated mitochondria under specific in vitro conditions, including the use of inhibitors of the ETC, which may not reflect the physiological situation in intact cells. Within the cellular lattice of intact myocytes, close association of mitochondria with Ca^{2+} stores and ATP-consuming sites (so-called microdomains) plays a key role in Ca^{2+}- and ADP-mediated regulation of mitochondrial function.[38,39] Furthermore, because the heart never stops beating, there is always a certain level of ADP-induced respiration, and thus, pure state 4 respiration never occurs.[14] Therefore, in the present study, we analyzed ROS production under more physiological conditions (ie, during state 3 respiration), with mitochondria spatially and functionally integrated into their native environment.

Using a novel technique in which patch clamping was combined with fluorescence microscopy in working myocytes, we observed that initiation of work (imposed by EC coupling) increased mitochondrial ROS production. Although this is in contrast to what would be expected from results on isolated mitochondria,[2,35–37] it is in line with a report on intact cardiac myocytes, in which an increase of the stimulation frequency potentiated intracellular ROS production.[40] Furthermore, we observed an inverse relation between the redox state of NAD(P)H and mitochondrial net formation of H_2O_2 (Figure 4F). Again, this is in contrast to results from isolated mitochondria, in which under state 4 conditions, the redox state of NAD(P)H correlated positively with ROS formation,[37] but it is in line with our previous observations in quiescent cardiac myocytes, where rapid dissipations of the mitochondrial membrane potential ($\Delta\Psi_m$) resulted in oxidation of NAD(P)H and increased ROS production.[27] In the latter study, the increase in ROS production was related to acceleration of electron flow through the ETC and thus an increased turnover rate in the Q cycle of complex III, a major source of $^{\bullet}O_2^-$ in mitochondria.[27] Accordingly, in the present study, ROS production was accelerated when the ETC was uncoupled with FCCP [carbonyl cyanide 4-(trifluoromethoxy)phenylhydrazone], which results in increased electron flux along the ETC until NADH is completely consumed, but it was reduced when electron flux was blocked by cyanide (online-only Data Supplement Figure III).

One major conclusion derived from the present experiments is that in working myocytes, ROS formation not only depends on the rate of electron flux along the ETC but is also dynamically regulated by the redox state of the mitochondrial matrix. Although the amplitude of $[Ca^{2+}]_c$ transients (which correlates with the amount of work and thus electron flux along the ETC[14]) was comparable 1 and 4 minutes after isoproterenol application (ie, at minutes 6 and 9 of the protocol in Figure 3B), net H_2O_2 formation was substantially higher at the earlier time point, when NAD(P)H was more oxidized (Figure 3G). Because the elimination of H_2O_2 is governed by peroxiredoxin and glutathione peroxidase, which require electrons from reduced NAD(P)H and glutathione, respectively (Figure 1),[25] these results suggest that fluctuations in the NAD(P)H/$NAD(P)^+$ redox state translate into variations in the antioxidative capacity of the matrix and thus net H_2O_2 formation. These conclusions are supported by our previous observations in quiescent cardiac myocytes, in which NAD(P)H correlated positively with the glutathione redox state but inversely with ROS formation.[26] Inhibition of the nicotinamide nucleotide transhydrogenase or glutathione reductase, 2 key enzymes that mediate electron and proton transfer from NADH to NADPH and from NADPH to glutathione, respectively (Figure 1), potentiated the formation of H_2O_2.[26] Also in isolated mitochondria, the glutathione redox state correlated closely with net H_2O_2 formation.[41]

After the initial oxidation of NAD(P)H to $NAD(P)^+$, the subsequent recovery of NAD(P)H was causally linked to progressive mitochondrial Ca^{2+} accumulation, because inhibition of the MCU blunted this recovery. In line with the inverse correlation between NAD(P)H and H_2O_2, blocking mitochondrial Ca^{2+} uptake potentiated net H_2O_2 formation. These data indicate that mitochondrial Ca^{2+} uptake is not only important for matching energy supply and demand but also for the recovery of the antioxidative capacity of the mitochondrial matrix to control net formation of H_2O_2. The close link between mitochondrial Ca^{2+} uptake and H_2O_2 formation is readily explained by the observations that (1) mitochondrial Ca^{2+} uptake accelerates the turnover rate of the Krebs cycle by stimulating rate-limiting dehydrogenases,[15–17] and (2) the regeneration of antioxidative enzymes depends on NADPH, which in turn is regenerated by substrates derived from the Krebs cycle (Figure 1).[25,26]

Regulation of H_2O_2 by $[Na^+]_i$

In heart failure, $[Na^+]_i$ is elevated,[20–22] which favors mitochondrial Ca^{2+} export via the mNCE, reduces steady state $[Ca^{2+}]_m$, and oxidizes NAD(P)H.[17,24] In the present study, ROS formation was increased substantially in failing compared with nonfailing myocytes. Of note, this difference occurred only in working but not quiescent myocytes. An inhibitor of the mNCE, which blocks Na^+-induced Ca^{2+} exportation and thus potentiates mitochondrial Ca^{2+} accumulation in failing and nonfailing myocytes,[17,24] prevented increased ROS formation. Moreover, sole elevation of $[Na^+]_i$ in normal myocytes per se potentiated ROS formation, whereas lowering $[Na^+]_i$ in failing myocytes prevented it. Thus, it can be concluded that elevated $[Na^+]_i$ and deficient mitochondrial Ca^{2+} uptake contribute to increased ROS formation in failing myocytes.

Besides the difference in $[Na^+]_i$, other factors may contribute to reduced mitochondrial Ca^{2+} uptake or increased ROS formation in failing myocytes. In a recent patch-clamp study on isolated mitochondria, the activity of mitochondrial Ca^{2+} channels (termed mCa1 and mCa2) was decreased in mitochondria from failing compared with nonfailing human myocardium.[42] Furthermore, $\Delta\Psi_m$, the driving force for mitochondrial Ca^{2+} uptake via the MCU (or mCa1/mCa2,[42] respectively), was decreased in mitochondria from failing hearts.[43] All of these changes in concert would predict deficient mitochondrial Ca^{2+} uptake in heart failure and, according to the present results, could potentiate mitochondrial ROS production.

Pathophysiological Implications and Conclusions

H_2O_2 activates the late Na^+ current (I_{Na}) and increases $[Na^+]_i$ in cardiac myocytes.[44] One potential mechanism for this activation is that Ca^{2+}/calmodulin kinase II is activated by ROS-induced methionine oxidation,[10] and Ca^{2+}/calmodulin kinase II interacts with the Na^+ channel, increasing late I_{Na} and $[Na^+]_i$.[45] Thus, in heart failure, a vicious circle of elevated $[Na^+]_i$ and oxidative stress may be established. Together with ROS-induced inhibition of sarcoplasmic reticulum Ca^{2+} ATPase,[6] activation of ryanodine receptors,[7] and the sarcolemmal Na^+/Ca^{2+} exchanger (in its reverse mode),[46] this vicious circle may sustain defects of EC coupling typically observed in heart failure.

In conclusion, we have identified a previously unrecognized role of mitochondrial Ca^{2+} uptake for the control of mitochondrial H_2O_2 levels and revealed a pathophysiological mechanism by which elevated $[Na^+]_i$ increases mitochondrial H_2O_2 in myocytes (Figure 1). Given that in addition to their negative effects on EC coupling and energetics,[6,7,10,27,44–46] mitochondrial ROS trigger apoptosis[12] and cardiac arrhythmias,[9] and given that oxidative stress has been linked to cardiac remodeling by inducing hypertrophic growth through activation of MAP kinases,[1] Ca^{2+}/calmodulin kinase II,[10] and histone-deacetylase 4,[11] therapeutic strategies aimed at correcting $[Na^+]_i$ or mitochondrial Ca^{2+} uptake in heart failure may be beneficial via a reduction in oxidative stress. Finally, this mechanism may also be of relevance for ischemia/reperfusion, during which a massive $[Na^+]_i$ overload occurs[23] and oxidative stress and cell death develop.

CLINICAL PERSPECTIVE

Oxidative stress plays a fundamental role in cardiovascular diseases and aging. In patients with heart failure, oxidative stress is causally linked to the progression of the disease, and mitochondria were identified as critical sources of reactive oxygen species (ROS) in the heart. ROS impair cardiac contractility, cause arrhythmias, and contribute to cardiac remodeling by inducing hypertrophy, apoptosis, and necrosis. The precise mechanisms that regulate mitochondrial ROS formation, however, are incompletely understood. Here, we identified a mechanism by which an elevation of cytosolic sodium ($[Na^+]_i$), as occurs in failing cardiac myocytes, increases mitochondrial ROS formation. A key role is played by the Krebs cycle, which produces NADH, the main electron donor for ATP production at the respiratory chain. A less appreciated role of the Krebs cycle, however, is to indirectly support the regeneration of NADPH, which serves to maintain the antioxidative capacity of the mitochondrial matrix. During transitions of workload (eg, during β-adrenergic stimulation), mitochondrial Ca^{2+} uptake activates rate-controlling enzymes of the Krebs cycle to adapt NADH production to an increased energetic demand. The elevated $[Na^+]_i$ in failing myocytes induces Ca^{2+} exportation from mitochondria via an Na^+/Ca^{2+} exchanger, which hampers regeneration of NADH and NADPH, resulting in energetic mismatch and oxidative stress. The effects of cytosolic Na^+ on mitochondrial function described in the present study indicate that this mechanism could play a role in the toxicity of cardiac glycosides (which further increase $[Na^+]_i$) and suggest a potential therapeutic application for drugs that lower $[Na^+]_i$ during the progression of heart failure.

Supplementary Material

Refer to Web version on PubMed Central for supplementary material.

Acknowledgments

We thank Michelle Gulentz and Angela Zimmer for technical assistance, Stefan Gräber for statistical consultation, and Sonia Cortassa, Miguel Aon, and Ulrich Laufs for discussion of the manuscript.

Sources of Funding

The study was supported by the Emmy Noether Program and the Klinische Forschergruppe KFO-196 by the Deutsche Forschungsgemeinschaft (to Dr Maack). Dr O'Rourke and Dr Liu are supported by the National Institutes of Health (P01-HL081427).

References

1. Giordano FJ. Oxygen, oxidative stress, hypoxia, and heart failure. J Clin Invest 2005;115:500–508. [PubMed: 15765131]
2. Balaban RS, Nemoto S, Finkel T. Mitochondria, oxidants, and aging. Cell 2005;120:483–495. [PubMed: 15734681]
3. Nakamura R, Egashira K, Machida Y, Hayashidani S, Takeya M, Utsumi H, Tsutsui H, Takeshita A. Probucol attenuates left ventricular dysfunction and remodeling in tachycardia-induced heart failure: roles of oxidative stress and inflammation. Circulation 2002;106:362–367. [PubMed: 12119254]
4. Li Y, Huang TT, Carlson EJ, Melov S, Ursell PC, Olson JL, Noble LJ, Yoshimura MP, Berger C, Chan PH, Wallace DC, Epstein CJ. Dilated cardiomyopathy and neonatal lethality in mutant mice lacking manganese superoxide dismutase. Nat Genet 1995;11:376–381. [PubMed: 7493016]
5. Ide T, Tsutsui H, Kinugawa S, Utsumi H, Kang D, Hattori N, Uchida K, Arimura K, Egashira K, Takeshita A. Mitochondrial electron transport complex I is a potential source of oxygen free radicals in the failing myocardium. Circ Res 1999;85:357–363. [PubMed: 10455064]
6. Zweier JL, Talukder MA. The role of oxidants and free radicals in reperfusion injury. Cardiovasc Res 2006;70:181–190. [PubMed: 16580655]
7. Yan Y, Liu J, Wei C, Li K, Xie W, Wang Y, Cheng H. Bidirectional regulation of Ca^{2+} sparks by mitochondria-derived reactive oxygen species in cardiac myocytes. Cardiovasc Res 2008;77:432–441. [PubMed: 18006452]
8. Maack C, Dabew ER, Hohl M, Schäfers HJ, Böhm M. Endogenous activation of mitochondrial KATP channels protects human failing myocardium from hydroxyl radical-induced stunning. Circ Res 2009;105:811–817. [PubMed: 19729596]
9. Akar FG, Aon MA, Tomaselli GF, O'Rourke B. The mitochondrial origin of postischemic arrhythmias. J Clin Invest 2005;115:3527–3535. [PubMed: 16284648]
10. Erickson JR, Joiner ML, Guan X, Kutschke W, Yang J, Oddis CV, Bartlett RK, Lowe JS, O'Donnell SE, Aykin-Burns N, Zimmerman MC, Zimmerman K, Ham AJ, Weiss RM, Spitz DR, Shea MA, Colbran RJ, Mohler PJ, Anderson ME. A dynamic pathway for calcium-independent activation of CaMKII by methionine oxidation. Cell 2008;133:462–474. [PubMed: 18455987]
11. Ago T, Liu T, Zhai P, Chen W, Li H, Molkentin JD, Vatner SF, Sadoshima J. A redox-dependent pathway for regulating class II HDACs and cardiac hypertrophy. Cell 2008;133:978–993. [PubMed: 18555775]
12. Giorgio M, Migliaccio E, Orsini F, Paolucci D, Moroni M, Contursi C, Pelliccia G, Luzi L, Minucci S, Marcaccio M, Pinton P, Rizzuto R, Bernardi P, Paolucci F, Pelicci PG. Electron transfer between cytochrome c and p66Shc generates reactive oxygen species that trigger mitochondrial apoptosis. Cell 2005;122:221–233. [PubMed: 16051147]
13. Halestrap A. Biochemistry: a pore way to die. Nature 2005;434:578–579. [PubMed: 15800609]
14. Balaban RS. Domestication of the cardiac mitochondrion for energy conversion. J Mol Cell Cardiol 2009;46:832–841. [PubMed: 19265699]
15. Brandes R, Bers DM. Intracellular Ca^{2+} increases the mitochondrial NADH concentration during elevated work in intact cardiac muscle. Circ Res 1997;80:82–87. [PubMed: 8978326]
16. Maack C, O'Rourke B. Excitation-contraction coupling and mitochondrial energetics. Basic Res Cardiol 2007;102:369–392. [PubMed: 17657400]
17. Maack C, Cortassa S, Aon MA, Ganesan AN, Liu T, O'Rourke B. Elevated cytosolic Na^+ decreases mitochondrial Ca^{2+} uptake during excitation-contraction coupling and impairs energetic adaptation in cardiac myocytes. Circ Res 2006;99:172–182. [PubMed: 16778127]
18. Houser SR, Margulies KB. Is depressed myocyte contractility centrally involved in heart failure? Circ Res 2003;92:350–358. [PubMed: 12623873]

19. Bers DM. Altered cardiac myocyte ca regulation in heart failure. Physiology (Bethesda) 2006;21:380–387. [PubMed: 17119150]
20. Despa S, Islam MA, Weber CR, Pogwizd SM, Bers DM. Intracellular Na^+ concentration is elevated in heart failure but Na/K pump function is unchanged. Circulation 2002;105:2543–2548. [PubMed: 12034663]
21. Pieske B, Maier LS, Piacentino V III, Weisser J, Hasenfuss G, Houser S. Rate dependence of [Na+]i and contractility in nonfailing and failing human myocardium. Circulation 2002;106:447–453. [PubMed: 12135944]
22. Baartscheer A, Schumacher CA, Belterman CN, Coronel R, Fiolet JW. [Na+]i and the driving force of the Na^+/Ca^{2+}-exchanger in heart failure. Cardiovasc Res 2003;57:986–995. [PubMed: 12650876]
23. Murphy E, Eisner DA. Regulation of intracellular and mitochondrial sodium in health and disease. Circ Res 2009;104:292–303. [PubMed: 19213964]
24. Liu T, O'Rourke B. Enhancing mitochondrial Ca^{2+} uptake in myocytes from failing hearts restores energy supply and demand matching. Circ Res 2008;103:279–288. [PubMed: 18599868]
25. Ying W. NAD+/NADH and NADP+/NADPH in cellular functions and cell death: regulation and biological consequences. Antioxid Redox Signal 2008;10:179–206. [PubMed: 18020963]
26. Aon MA, Cortassa S, Maack C, O'Rourke B. Sequential opening of mitochondrial ion channels as a function of glutathione redox thiol status. J Biol Chem 2007;282:21889–21900. [PubMed: 17540766]
27. Aon MA, Cortassa S, Marban E, O'Rourke B. Synchronized whole cell oscillations in mitochondrial metabolism triggered by a local release of reactive oxygen species in cardiac myocytes. J Biol Chem 2003;278:44735–44744. [PubMed: 12930841]
28. Kirichok Y, Krapivinsky G, Clapham DE. The mitochondrial calcium uniporter is a highly selective ion channel. Nature 2004;427:360–364. [PubMed: 14737170]
29. Cox DA, Matlib MA. A role for the mitochondrial Na^+-Ca^{2+} exchanger in the regulation of oxidative phosphorylation in isolated heart mitochondria. J Biol Chem 1993;268:938–947. [PubMed: 8419373]
30. Belch JJ, Bridges AB, Scott N, Chopra M. Oxygen free radicals and congestive heart failure. Br Heart J 1991;65:245–248. [PubMed: 2039668]
31. Maack C, Kartes T, Kilter H, Schäfers HJ, Nickenig G, Böhm M, Laufs U. Oxygen free radical release in human failing myocardium is associated with increased activity of rac1-GTPase and represents a target for statin treatment. Circulation 2003;108:1567–1574. [PubMed: 12963641]
32. Valgimigli M, Merli E, Malagutti P, Soukhomovskaia O, Cicchitelli G, Antelli A, Canistro D, Francolini G, Macri G, Mastrorilli F, Paolini M, Ferrari R. Hydroxyl radical generation, levels of tumor necrosis factor-alpha, and progression to heart failure after acute myocardial infarction. J Am Coll Cardiol 2004;43:2000–2008. [PubMed: 15172404]
33. Takemoto M, Node K, Nakagami H, Liao Y, Grimm M, Takemoto Y, Kitakaze M, Liao JK. Statins as antioxidant therapy for preventing cardiac myocyte hypertrophy. J Clin Invest 2001;108:1429–1437. [PubMed: 11714734]
34. Bendall JK, Cave AC, Heymes C, Gall N, Shah AM. Pivotal role of a gp91(phox)-containing NADPH oxidase in angiotensin II-induced cardiac hypertrophy in mice. Circulation 2002;105:293–296. [PubMed: 11804982]
35. Turrens JF. Mitochondrial formation of reactive oxygen species. J Physiol 2003;552:335–344. [PubMed: 14561818]
36. Korshunov SS, Skulachev VP, Starkov AA. High protonic potential actuates a mechanism of production of reactive oxygen species in mitochondria. FEBS Lett 1997;416:15–18. [PubMed: 9369223]
37. Starkov AA, Fiskum G. Regulation of brain mitochondrial H_2O_2 production by membrane potential and NAD(P)H redox state. J Neurochem 2003;86:1101–1107. [PubMed: 12911618]
38. Rizzuto R, Pozzan T. Microdomains of intracellular Ca^{2+}: molecular determinants and functional consequences. Physiol Rev 2006;86:369–408. [PubMed: 16371601]
39. Saks V, Dzeja P, Schlattner U, Vendelin M, Terzic A, Wallimann T. Cardiac system bioenergetics: metabolic basis of the Frank-Starling law. J Physiol 2006;571:253–273. [PubMed: 16410283]
40. Heinzel FR, Luo Y, Dodoni G, Boengler K, Petrat F, Di Lisa F, de Groot H, Schulz R, Heusch G. Formation of reactive oxygen species at increased contraction frequency in rat cardiomyocytes. Cardiovasc Res 2006;71:374–382. [PubMed: 16780821]

41. Han D, Canali R, Rettori D, Kaplowitz N. Effect of glutathione depletion on sites and topology of superoxide and hydrogen peroxide production in mitochondria. Mol Pharmacol 2003;64:1136–1144. [PubMed: 14573763]

42. Michels G, Khan IF, Endres-Becker J, Rottlaender D, Herzig S, Ruhparwar A, Wahlers T, Hoppe UC. Regulation of the human cardiac mitochondrial Ca^{2+} uptake by 2 different voltage-gated Ca^{2+} channels. Circulation 2009;119:2435–2443. [PubMed: 19398664]

43. Lin L, Sharma VK, Sheu SS. Mechanisms of reduced mitochondrial Ca^{2+} accumulation in failing hamster heart. Pflugers Arch 2007;454:395–402. [PubMed: 17387508]

44. Song Y, Shryock JC, Wagner S, Maier LS, Belardinelli L. Blocking late sodium current reduces hydrogen peroxide-induced arrhythmogenic activity and contractile dysfunction. J Pharmacol Exp Ther 2006;318:214–222. [PubMed: 16565163]

45. Wagner S, Dybkova N, Rasenack EC, Jacobshagen C, Fabritz L, Kirchhof P, Maier SK, Zhang T, Hasenfuss G, Brown JH, Bers DM, Maier LS. Ca^{2+}/calmodulin-dependent protein kinase II regulates cardiac Na^{+} channels. J Clin Invest 2006;116:3127–3138. [PubMed: 17124532]

46. Zeitz O, Maass AE, Van Nguyen P, Hensmann G, Kögler H, Möller K, Hasenfuss G, Janssen PM. Hydroxyl radical-induced acute diastolic dysfunction is due to calcium overload via reverse-mode Na^{+}-Ca^{2+} exchange. Circ Res 2002;90:988–995. [PubMed: 12016265]

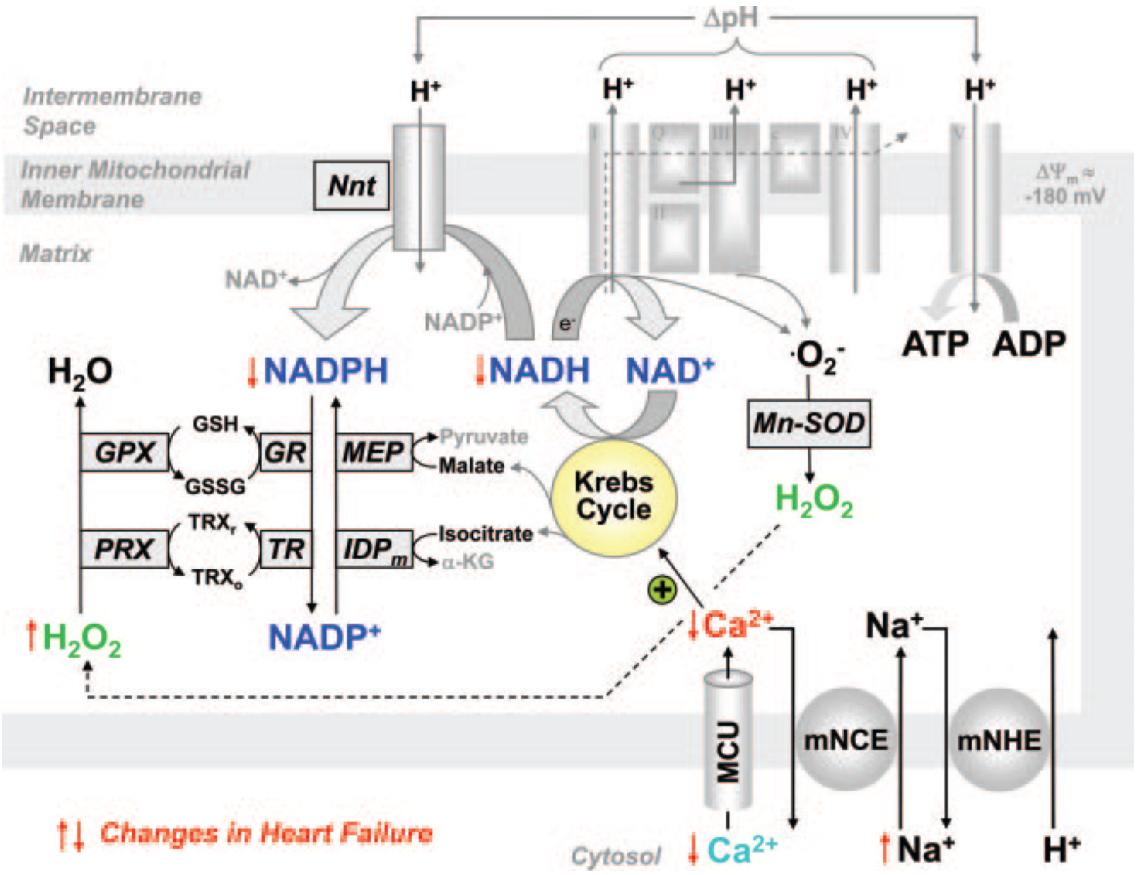

Figure 1.

Regulation of oxidative phosphorylation and ROS formation by NAD(P)H and Ca^{2+}. The Krebs cycle is fueled by metabolic substrates (glucose, fatty acids) via acetyl-coenzyme A and mediates the recovery of oxidized NAD^+ to NADH, which donates electrons to the ETC for oxidative phosphorylation of ATP. Regeneration of antioxidative capacity is also coupled to the Krebs cycle, because regeneration of NADPH requires products of the Krebs cycle (isocitrate, malate, NADH). Three rate-controlling enzymes of the Krebs cycle (pyruvate, isocitrate, and α-ketoglutarate dehydrogenase) are activated by Ca^{2+}. $\Delta\Psi_m$ indicates mitochondrial membrane potential; Nnt, nicotinamide nucleotide transhydrogenase; Mn-SOD, Mn^{2+}-dependent superoxide dismutase; PRX, peroxiredoxin; GPX, glutathione peroxidase; $TRX_{r/o}$, reduced/oxidized thioredoxin; GSH/GSSG, reduced/oxidized glutathione; TR, thioredoxin reductase; GR, glutathione reductase; IDP_m, mitochondrial $NADP^+$-dependent isocitrate dehydrogenase; MEP, mitochondrial malic enzyme; α-KG, α-ketoglutarate; and mNHE, mitochondrial Na^+/H^+ exchanger.

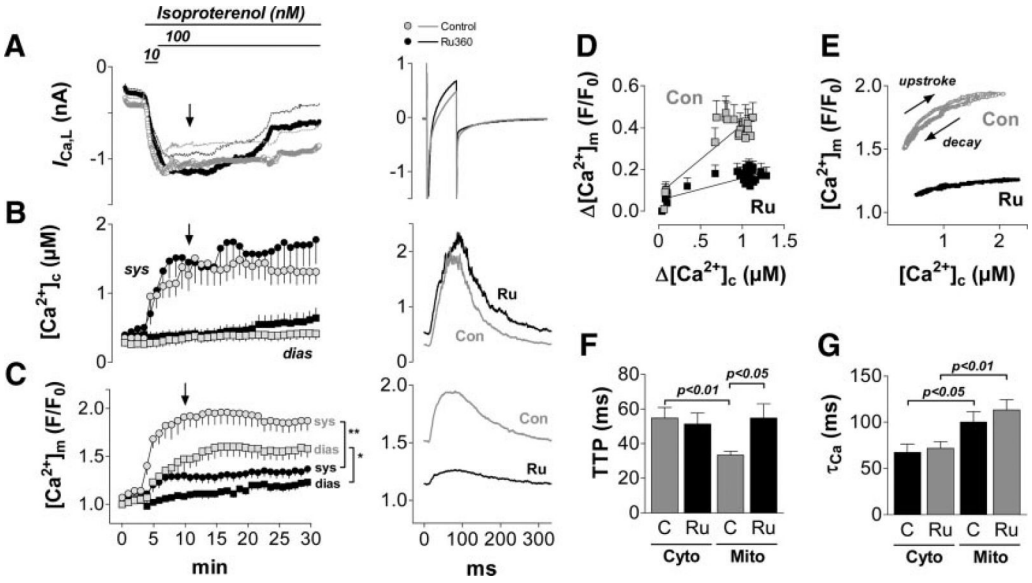

Figure 2.

Mitochondrial Ca^{2+} uptake during transitions of workload. Myocytes were depolarized from −80 to 10 mV for 80 ms at 3 Hz and superfused with isoproterenol. Pipette solution contained 5 mmol/L $[Na^+]_i$, in the absence (control, n=13) and presence of the MCU-blocker Ru360 (1 μmol/L; n=11). A–C, left panels: Time courses of L-type Ca^{2+} currents ($I_{Ca,L}$; A), $[Ca^{2+}]_c$ (B), and $[Ca^{2+}]_m$ (C) during the whole experiment; right panels, averaged currents, $[Ca^{2+}]_c$, and $[Ca^{2+}]_m$ after 10 minutes of the protocol, respectively (see arrow in left panels). Con indicates control; sys, systole; and dias, diastole. D, Averaged amplitudes of $[Ca^{2+}]_m$ ($\Delta[Ca^{2+}]_m$) plotted against the respective $\Delta[Ca^{2+}]_c$, in the absence (Con) and presence of Ru360 (Ru). E, $[Ca^{2+}]_m$ plotted against $[Ca^{2+}]_c$ during a single Ca^{2+} transient (averaged data at 10 minutes of the protocol). F, Time to peak (TTP) and G, time constant of decay (τ) of $[Ca^{2+}]_c$ (Cyto) and $[Ca^{2+}]_m$ (Mito) in the absence (C) and presence (Ru) of Ru360, respectively. *P<0.05 from minute 9 to 12 and P<0.01 from minute 12 to 30; **P<0.01 from minute 6 to 30 in C, and as indicated in F and G (2-way ANOVA, respectively).

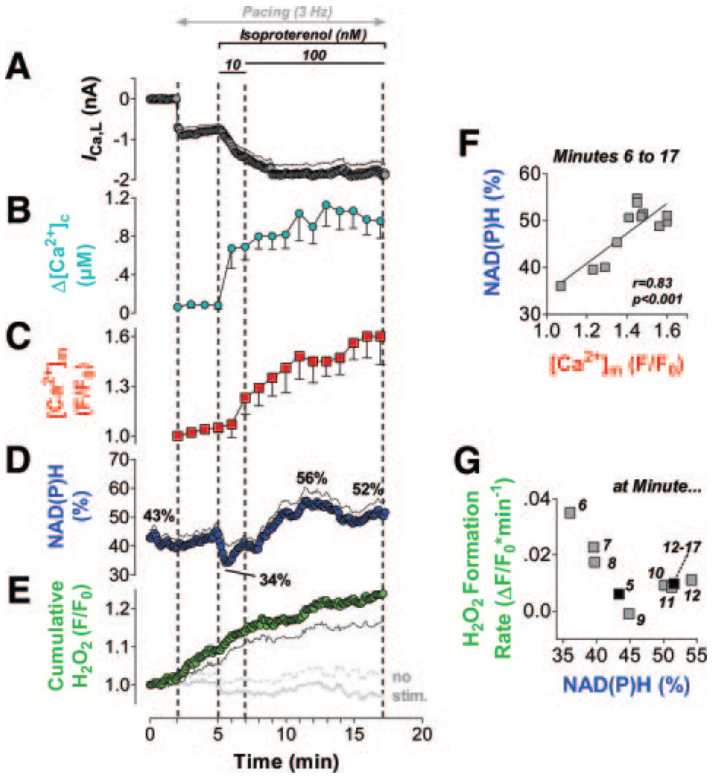

Figure 3.

Dynamic regulation of mitochondrial ROS by $[Ca^{2+}]_m$ and NAD(P)H. Myocytes (n=16) were loaded with CM-H_2DCF to monitor H_2O_2 together with the autofluorescence of NAD(P)H. A similar protocol as in Figure 2 was performed (voltage-clamp pulses from −80 to 10 mV at 3 Hz, $[Na^+]_i$=5 mmol/L). Changes in $I_{Ca,L}$ (A), NAD(P)H (D), and H_2O_2 (E) are displayed together with changes in $\Delta[Ca^{2+}]_c$ (B) and diastolic $[Ca^{2+}]_m$ (C) from the experiments in Figure 2 (control group). The gray trace in E indicates H_2O_2 in unpatched cells that were not paced. F, NAD(P)H correlated to diastolic $[Ca^{2+}]_m$ after β-adrenergic stimulation and initial NAD(P)H oxidation (starting at minute 6). G, Rates of CM-DCF oxidation, indicating the net H_2O_2 formation ($\Delta F/F_0 \times min^{-1}$), averaged over 1 minute, respectively, and correlated to the respective (averaged) NAD(P)H levels after β-adrenergic stimulation with isoproterenol at the indicated time points. For minutes 12 to 17, 1 average value was calculated. Stim indicates stimulation.

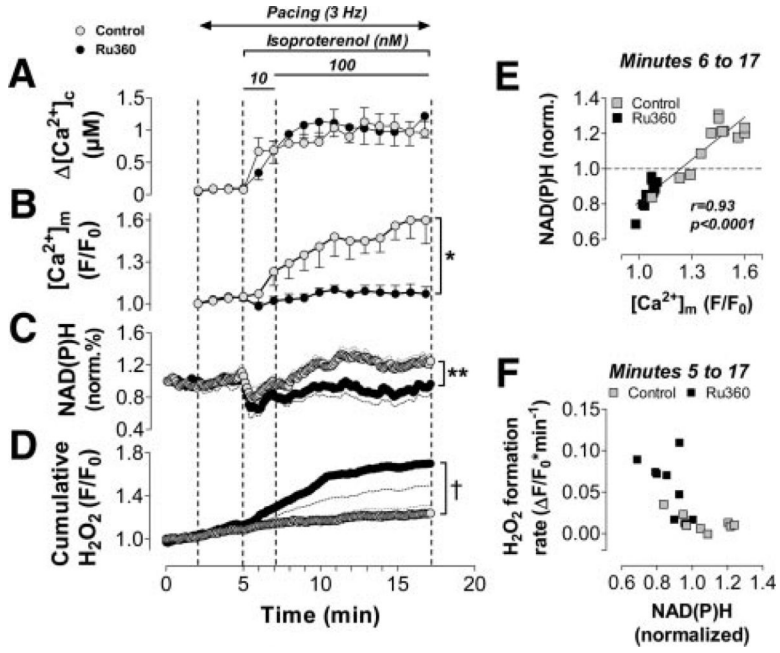

Figure 4.

Inhibition of mitochondrial Ca^{2+} uptake increases mitochondrial ROS production. The same protocol was used as in Figures 2 and 3, respectively. Amplitudes of $[Ca^{2+}]_c$ ($\Delta[Ca^{2+}]_c$; A) and diastolic $[Ca^{2+}]_m$ (B), in the absence (Con, n=13) and presence (Ru, n=11; 1 μmol/L in the pipette solution) of Ru360 are displayed. Ca^{2+} data are taken from the series of experiments in Figure 2. NAD(P)H (C) and H_2O_2 (D) in the absence (n=16) and presence of Ru360 (n=15; 1 μmol/L in the pipette solution). E, NAD(P)H plotted against diastolic $[Ca^{2+}]_m$. F, Net mitochondrial formation of H_2O_2 plotted versus NAD(P)H. *P<0.05 at minute 8 to 10 and P<0.01 from minute 12 to 17; **P<0.05 from minute 10 to 15; †P<0.05 at minute 14 to 17 and P<0.07 at minute 7 to 14 (1-way ANOVA, respectively).

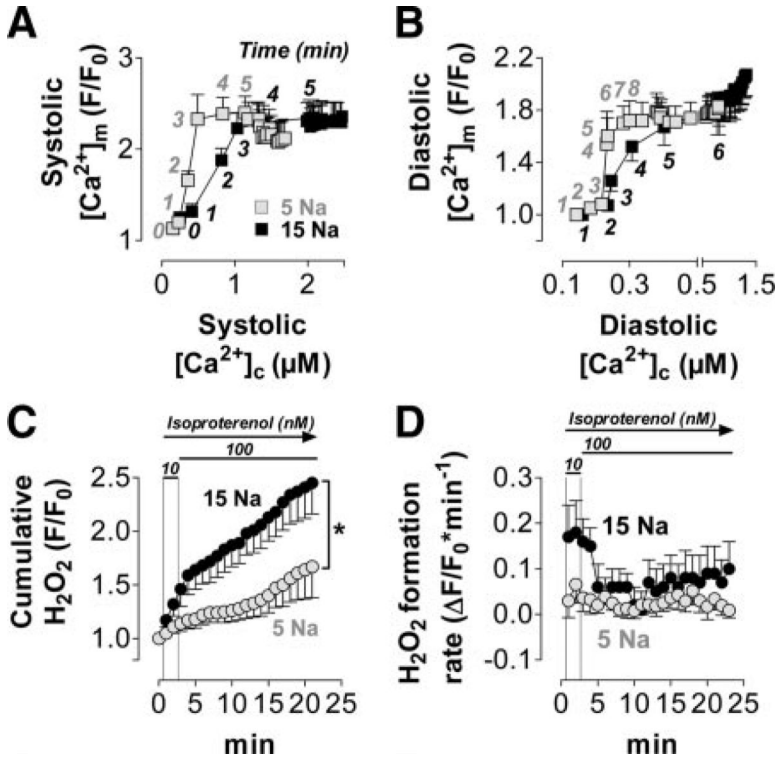

Figure 5.

Elevated $[Na^+]_i$ increases ROS production in normal myocytes. A similar protocol as in Figure 2 was performed, except that isoproterenol was washed in starting 40 seconds after the onset of pacing. Pipette solution was 5 or 15 mmol/L $[Na^+]_i$ as indicated. A and B, $[Ca^{2+}]_c$ and $[Ca^{2+}]_m$ were measured in normal myocytes (5 mmol/L $[Na^+]_i$, n=15; 15 mmol/L $[Na^+]_i$, n=20). A, Systolic $[Ca^{2+}]_m$ plotted against systolic $[Ca^{2+}]_c$; B, diastolic $[Ca^{2+}]_m$ plotted against diastolic $[Ca^{2+}]_c$; the numbers indicate the time (in minutes) after the start of the experiment. C and D, Net H_2O_2 formation was determined by CM-DCF in a separate set of cells (n=15/12). CM-DCF oxidation, indicating levels of H_2O_2, is given as F/F_0 (C) or $\Delta F/F_0$ per minute (D). **P*<0.05 for 5 vs 15 mmol/L $[Na^+]_i$ at minute 6 to 18 (1-way ANOVA).

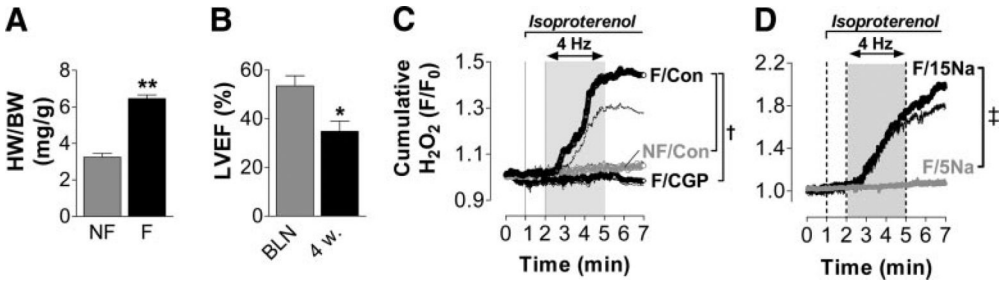

Figure 6.

Increased ROS production in failing myocytes is related to deficient mitochondrial Ca^{2+} uptake. A, Heart weight/body weight (HW/BW) ratio in guinea pigs 4 weeks after ascending aortic constriction (failing, F; n=3) compared with age- and sex-matched control animals (nonfailing, NF; n=4). B, In vivo left ventricular ejection fraction (LVEF) before (BLN) and 4 weeks after (4w) aortic banding (n=3). C, H_2O_2 levels in intact, field-stimulated myocytes (4 Hz) from normal (NF, n=8) or failing (F) myocytes, in the absence (Con; n=8) or presence (CGP) of CGP-37157 (1 μmol/L; n=6), an inhibitor of the mNCE. D, Cumulative H_2O_2 formation in failing myocytes that were voltage clamped (4 Hz) and equilibrated with a pipette solution that contained either 5 or 15 mmol/L $[Na^+]$ (n=7/3). *P<0.05 F vs NF; **P<0.01 4w vs BLN; †P<0.05 F/Con vs NF/Con and F/CGP vs F/Con at minutes 4 to 7, respectively; ‡P<0.001 for 5 vs 15 mmol/L $[Na^+]_i$ at minutes 3 to 7 by unpaired t test (A), paired t test (B), and 1-way ANOVA (C and D), respectively.